This is the accepted version of the following article: Olazabal-Herrero, A., García-Santisteban, I. and Rodríguez, J.A. (2016), *Mutations in the 'Fingers' subdomain of the deubiquitinase USP1 modulate its function and activity*. **FEBS J**, 283: 929-946, which has been published in final form at https://doi.org/10.1111/febs.13648.

Author Manuscript

Color: Fig1-7

Mutations in the 'Fingers' subdomain of the deubiquitinase USP1 modulate its function and activity

Anne Olazabal-Herrero, Iraia García-Santisteban[#], Jose Antonio Rodríguez[*].

Department of Genetics, Physical Anthropology and Animal Physiology, University of the Basque Country (UPV/EHU), Leioa, Spain.

[#]Current Address: Division of Cell Biology I, The Netherlands Cancer Institute, Amsterdam, The Netherlands.

*Corresponding author: Jose Antonio Rodríguez.

Fax: +34946013145

Telephone: +34946018072

E-mail: josean.rodriguez@ehu.es

Running title:

GENERAL UBIQUITIN DECONJUGATION BY USP1/UAF1

Abbreviations:

ATM: Ataxia Telangiectasia Mutated; DDR: DNA Damage Response; DSB: Double Strand Break; DUB: Deubiquitinating Enzyme; FA: Fanconi Anemia; FANCD2: Fanconi anemia

This is the author manuscript accepted for publication and has undergone full peer review but has not been through the copyediting, typesetting, pagination and proofreading process, which may lead to differences between this version and the Version of Record. Please cite this article as doi: 10.1111/febs.13648

This article is protected by copyright. All rights reserved

group D2 protein; GFP: Green Fluorescent Protein; HPV11: Human Papillomavirus 11; HU: Hydroxyurea; H3K4Me3: Lys4-trimethylated Histone H3; H3K9Me3: Lys9-trimethylated Histone H3; H3K56Ac: Lys56-acetylated Histone H3; ICL: Interstrand DNA crosslink; ID: Inhibitors of DNA binding; MDC1: Mediator of DNA damage Checkpoint protein 1; MMS: Methyl methanesulfonate; NCS: Neocarzinostatin; NLS: Nuclear Localization Signal; PCNA: Proliferating Cell Nuclear Antigen; PTM: Post-Translational Modification; SEM: Standard Error of the Mean; SV40: Simian Virus 40; TLS: Translesion síntesis; UAF1: USP1-Associated Factor 1; Ub: Ubiquitin; USP: Ubiquitin Specific Protease; YFP: Yellow Fluorescent Protein; γH2AX: phosphorylated histone H2AX; 53BP1: p53 Binding Protein 1.

Keywords:

UBIQUITINATION, USP1, UAF1, DEUBIQUITINASE, DNA DAMAGE

ABSTRACT

USP1 is a member of the ubiquitin-specific protease (USP) family of deubiquitinating enzymes. Efficient USP1 activity requires binding to its cofactor UAF1, and the USP1/UAF1 deubiquitinase complex has important roles in regulating DNA damage-related processes. USPs exhibit a common folding of their catalytic domain with three subdomains termed Thumb, Palm and Fingers. The Fingers appears to be the primary site for ubiquitin binding. In USP1, the Fingers subdomain also mediates its interaction with UAF1 and thus represents a crucial, yet poorly characterized motif in USP1. To explore the role of USP1/UAF1 in ubiquitin-dependent nuclear processes, we tested the effect of modulating USP1/UAF1 activity on the level and/or localization of conjugated ubiquitin and the DNA damage-related proteins γH2AX, H3K56Ac and 53BP1. siRNA-mediated USP1 knockdown or treatment with the novel USP1/UAF1 inhibitor ML323 increased the recruitment of conjugated ubiquitin and 53BP1 into nuclear foci. Strikingly, ectopic coexpression of USP1 and UAF1 depleted conjugated ubiquitin in the nucleus and blocked the recruitment of 53BP1 to DNA damage foci. In a direct comparison with other overexpressed USPs, USP1/UAF1 behaved as a relatively promiscuous deubiquitinase. Experimental and cancer-related mutations in the USP1 Fingers subdomain abrogated substrate deubiquitination without interfering with other USP1 activities, such as UAF1 binding or autocleavage. These results bring new insight into the function and regulation of the USP1/UAF1 complex.

INTRODUCTION

This article is protected by copyright. All rights reserved

Author Manuscript

Living organisms can be exposed to a variety of endogenous and exogenous DNA damaging agents that generate genomic lesions. To preserve genome integrity, cells have evolved a complex array of mechanisms to detect, signal and repair DNA damage, which collectively constitute the so-called DNA damage response (DDR) [1]. In this cellular response, DNA damage induces a relocalization of multiple repair factors into nuclear foci at damage sites [2]. Recruitment of these factors is crucially regulated by a complex interplay of protein post-translational modifications (PTMs) [3]. In particular, the importance of protein ubiquitination in several key steps of the DDR is becoming increasingly clear [4].

Protein ubiquitination involves the sequential activity of three enzymes, an E1 (activating) enzyme, an E2 (conjugating) enzyme, and an E3 ubiquitin ligase. Proteins can be tagged at one or more lysine residues with a single ubiquitin molecule (monoubiquitinated), or with a chain of several ubiquitin moieties (polyubiquitinated) with variable length and linkage topology. Ubiquitin tags can be subsequently edited or removed by the activity of deubiquitinating enzymes (DUBs). The concerted action of E3 ligases and DUBs renders ubiquitin (de)conjugation a very complex and dynamic process that modulates the levels, localization and/or function of many cellular proteins [5].

Several E3 ubiquitin ligases and DUBs have been shown to play a role in DNA damage signaling and repair [6]. One of the first DUBs identified as a regulator of DDR was USP1, a member of the ubiquitin specific protease (USP) family. USP1 is a nuclear DUB whose catalytic activity requires allosteric activation through binding to its cofactor USP1-Associated Factor 1 (UAF1) [7]. UAF1 binding is also required by two other USP family members, USP12 and USP46, to be catalytically active [8]. The USP1/UAF1 complex has been firmly established as a key player in two DNA damage-related processes. On the one hand, it contributes to the repair of interstrand DNA crosslinks (ICLs) through the Fanconi anemia (FA) pathway, by reverting monoubiquitination of FANCD2 [9]. On the other hand, the USP1/UAF1 complex participates in translesion synthesis (TLS), a DNA damage tolerance mechanism, by reverting monoubiquitination of PCNA [10]. Besides these well-characterized functions, a potential role of USP1/UAF1 in additional aspects of the DDR is suggested by several lines of evidence. First, double knockout mice lacking both FANCD2 and USP1 exhibit a more severe phenotype than knockout mice lacking only USP1 [11]. Second, USP1/UAF1 promotes homologous recombination by a yet unknown mechanism that might be unrelated to the FA pathway [12]. Third, GFP-USP1 has been shown to be recruited to double-strand DNA breaks (DSBs) induced by laser micro-irradiation [13]. Furthermore, it is important to note that the function of USP1/UAF1 in the nucleus extends beyond its DDR-related roles to include deubiquitination of Inhibitors of DNA binding (ID) proteins that regulate differentiation processes [14]. Altogether, these findings suggest that the role of USP1/UAF1 as a regulator of nuclear protein ubiquitination deserves further investigation.

This article is protected by copyright. All rights reserved

Author Manuscript

Like many other proteins that participate in the DDR, USP1 is emerging as a potential target in cancer therapy [15]. Overexpression of USP1 is frequently observed in different types of cancer, and large-scale genomic analyses have uncovered USP1 gene mutations, albeit at a low frequency, in tumor samples [15]. Importantly, interfering with USP1 function in several experimental models has been reported to increase cellular sensitivity to a variety of chemotherapeutic drugs [11,12,16]. In this regard, a number of USP1/UAF1 small-molecule inhibitors have been recently developed [17,18,19]. ML323, the most specific USP1/UAF1 inhibitor reported up to date [20], constitutes an important tool to investigate USP1/UAF1 activity and, with further improvement of its pharmacodynamics and pharmacokinetics properties, might eventually undergo clinical development.

Clinical implementation of USP1-targeted therapies would greatly benefit from a deeper understanding of its basic biology, which is presently limited by the lack of a three dimensional structure of the USP/UAF1 complex. Based on the solved structures of several other USP family members [21,22,23], it has been determined that the catalytic domain of USPs shows a characteristic folding that resembles an open hand, with three subdomains termed Thumb, Palm and Fingers [24,25]. The Fingers subdomain appears to be the primary site for ubiquitin binding by USPs. Intriguingly, we have previously shown that the Fingers subdomain of USP1 and USP46 also mediates their binding to UAF1 [26]. Thus, this subdomain may be critical in regulating USP1/UAF1 activity. In the absence of specific structural information, combination of site-directed mutagenesis with functional assays may provide further information about how the function of the USP1/UAF1 complex is regulated and may be altered by experimentally-introduced and naturally occurring Fingers subdomain mutations.

In this report, we describe the effect that modulating USP1/UAF1 function has on the levels and localization of conjugated ubiquitin in the nucleus, as well as on the levels and localization of two proteins involved in the response to DSBs, phosphorylated histone H2AX (γH2AX), and p53 binding protein 1 (53BP1). Interfering with USP1/UAF1 function increased the number of nuclear ubiquitin-containing foci and 53BP1 foci. These findings provide further support to previously reported evidence suggesting that USP1/UAF1 may have additional DDR-related nuclear functions beyond those in FA and TLS. Most strikingly, we found that ectopic expression of USP1/UAF1 led to an apparently complete depletion of conjugated ubiquitin in the nucleus and blocked the recruitment of 53BP1 to DNA damage foci. We carried out a direct comparison of USP1/UAF1 with several other USPs using general ubiquitin deconjugation as cellular readout. The results of this comparison suggest a still unexplored wide range of substrate promiscuity in USP family DUBs. Finally, we used depletion of conjugated ubiquitin and blockade of 53BP1 foci formation as readouts to further validate ML323 as a USP1/UAF1 inhibitor and, together with previously described assays, to characterize in detail the phenotypic consequences of mutations in USP1 Fingers subdomain.

This article is protected by copyright. All rights reserved

Author Manuscript

RESULTS

Modulating USP1/UAF1 function affects general ubiquitin conjugation in the nucleus

General protein ubiquitination can be monitored in cells using immunofluorescence with the FK2 monoclonal antibody, a well-validated and widely-used reagent that specifically recognizes conjugated, but not free ubiquitin [27]. To further investigate the role of the USP1/UAF1 complex in regulating the ubiquitination of nuclear proteins, we carried out FK2 immunostaining in 293T cells in which the activity of this complex was modulated using different experimental approaches.

On the one hand, we interfered with the activity of USP1/UAF1 by using siRNA-based USP1 knockdown or by treating the cells with the recently described inhibitor ML323 [20]. USP1 knockdown was carried our using a pool of three siRNA oligonucleotides that consistently reduces USP1 mRNA (not shown) and protein levels (Figure 1A). As shown in Figure 1A, USP1 knockdown led to a significant increase in the percentage of cells having more than five FK2-positive foci in the nucleus. A similar but slightly more pronounced effect was observed in cells treated with ML323 (Figure 1B). On the other hand, we increased the cellular levels of the USP1/UAF1 complex by co-transfecting GFP-USP1 and Xpress-UAF1. In these experiments, a fusion of GFP to the SV40 nuclear localization signal (NLS-GFP) was included as a negative control. Image analysis was used to quantify the intensity of the FK2 immunofluorescence signal in transfected cells. Strikingly, overexpression of USP1/UAF1 resulted in a drastic reduction of the FK2 signal in the nucleus (Figure 1C). Importantly, the intensity of the FK2 signal was not reduced when GFP-USP1 was expressed alone, or when a catalytically inactive mutant GFP-USP1^{C90S} was co-expressed with UAF1.

Formation of ubiquitin-containing foci, reflecting the recruitment of ubiquitinated proteins to the sites of DNA damage, is a hallmark of the DDR [28] and the number of FK2-positive nuclear foci is well known to increase when cells are treated with agents that cause DSBs, such as the radiomimetic drug neocarzinostatin (NCS) [29,30,31,32]. In line with these reports, we found that nearly all 293T cells exhibited more than five FK2-positive foci after NCS treatment (not shown). We sought to determine if overexpression of USP1/UAF1 would interfere with the formation of NCS-induced FK2 foci. As previously observed in untreated cells, virtually no FK2 signal could be detected in NCS-treated cells overexpressing USP1/UAF1 (Figure 1D). In contrast, NCS-induced FK2 foci were readily detected in cells overexpressing the NLS-GFP control, GFP-USP1 alone or the catalytically inactive GFP-USP1^{C90S}.

These results indicate that interfering with USP1/UAF1 activity promotes the accumulation of ubiquitinated proteins into nuclear foci, whereas ectopic overexpression of the USP1/UAF1

This article is protected by copyright. All rights reserved

Author Manuscript

complex promotes general ubiquitin deconjugation, thus preventing formation of ubiquitin-containing foci in response to DSBs.

Modulating USP1/UAF1 function affects proteins that mediate the cellular response to DSBs

One of the first steps in the cellular response to DSBs, is the phosphorylation of the histone variant H2AX by Ataxia telangiectasia mutated (ATM)-related kinases [33,34]. Phosphorylated H2AX (γH2AX) accumulates into the sites of DNA damage, and facilitates the recruitment of Mediator of DNA damage checkpoint protein 1 (MDC1) [35]. This protein serves as a binding platform for the E3 ubiquitin ligases RNF8 [36,37] and RNF168 [38], which ubiquitinate histones H2A and γH2AX, thus promoting the ubiquitination-dependent recruitment of several DNA repair factors, including 53BP1 [39]. Interestingly, a previous large-scale siRNA screening has identified the DUBs USP1 and USP11 as two of 73 genes that regulate the cellular levels of γH2AX in untreated cells, and may participate in DDR signaling [40].

In order to further evaluate the possible effect that modulating USP1/UAF1 function might have on the cellular response to DSBs, we focused on γH2AX and 53BP1, an apical and a downstream factor, respectively, in the DSB response. As expected, both proteins readily accumulated into nuclear foci in NCS-treated 293T cells (not shown). We also investigated a potential effect of USP1/UAF1 on three other histone modifications, related to either DDR (H3K56Ac), or to active/repressive chromatin states (H3K4Me3 and H3K9Me3, respectively) [41].

USP1 has turned up in previous high throughput siRNA screens for genes modulating the levels of phosphorylated histone γH2AX [40,42]. In line with previous findings [40], siRNA-mediated knockdown of USP1 and USP11 in untreated 293T cells increased the nuclear levels of γH2AX (Figure 2A), although an increase in the number of γH2AX foci was not evident, in contrast to a previous report on the effect of USP11 silencing [43]. Overexpression of GFP-USP1 and Xpress-UAF1 did not interfere with the recruitment of γH2AX into NCS-induced nuclear foci, a phosphorylation-dependent event (Figure 2A). None of the other histone modifications tested was affected by modulating USP1/UAF1 levels. Thus, staining for H3K56Ac (Figure 2B), H3K4Me3 (Figure 2C) and H3K9Me3 (Figure 2D) remained unaltered in cells transfected with USP1 siRNA or overexpressing the USP1/UAF1 complex.

In the case of 53BP1, an increased number of nuclear foci was observed when the activity of the USP1/UAF1 complex was decreased by using either USP1 siRNA (Figure 2E) or ML323 treatment (Figure 2F), although only in the case of ML323-treated cells was the percentage of cells with more than five 53BP1 foci significantly higher than in control cells. Conversely, USP1/UAF1 overexpression (Figure 2G) completely blocked the recruitment of 53BP1 into NCS induced-foci, an ubiquitination-dependent event. Blockade of 53BP1 foci formation required co-expression of Xpress-UAF1, as well as USP1 catalytic activity.

This article is protected by copyright. All rights reserved

Author Manuscript

In summary, modulating USP1/UAF1 activity in cells affects the level or recruitment of DSB response-related proteins γH2AX and 53BP1.

A comparison of USP1/UAF1 with other nuclear USPs using depletion of conjugated ubiquitin as readout

The dramatic effect of USP1/UAF1 overexpression on nuclear ubiquitin conjugation prompted us to test the possibility that overexpression of other nuclear USP family DUBs might have a similar effect. *In vitro* analyses have shown that USP members are generally promiscuous in terms of the type of the ubiquitin linkage they can process [25,44], but little is known about their substrate promiscuity in a cellular context. We reasoned that the depletion of conjugated ubiquitin, as detected by FK2 immunofluorescence, could represent a useful cellular readout to gauge the relative substrate promiscuity of DUBs. In this regard, although FK2 immunostaining has been previously performed in cells overexpressing specific USPs, such as USP36 [45], USP29 and USP44 [46], USP16 [47], or USP26 and USP37 [48], a systematic comparison of how overexpression of different USP family DUBs affects FK2 signal has not yet been attempted, to the best of our knowledge.

To begin addressing this issue, we directly compared the levels of FK2 immunofluorescence signal in the nucleus of 293T cells overexpressing five different GFP- or YFP-tagged USPs (Figure 3A). Besides USP1, three nuclear USPs [USP3, USP7 and USP22) were tested. We also included USP46 in the analysis, as this DUB, like USP1, is activated by UAF1. Since USP46 is a cytoplasmic protein, a heterologous NLS was added to force its nuclear accumulation as previously described [26]. In these experiments, both GFP-USP1 and NLS-USP46-GFP were co-expressed with Xpress-UAF1 and NLS-GFP was used as a negative control. The intensity of FK2 immunofluorescence in the nucleus of cells expressing the different USPs was normalized using the FK2 intensity in the nucleus of non-transfected cells from the same sample as a reference. The relative FK2 intensity was then plotted against the intensity of the nuclear GFP/YFP fluorescence (Figure 3B).

Overexpression of the NLS-GFP control, NLS-USP46-GFP/UAF1, YFP-USP3 or YFP-USP22 did not affect FK2 immunostaining, even at high expression levels, while a partial decrease in the intensity of the FK2 signal was noted in cells expressing moderate-to-high levels of YFP-USP7. In the case of USP1/UAF1, a drastic reduction in FK2 signal was clearly evident even in cells expressing very low levels of GFP-USP1.

FK2 immunofluorescence was also carried out in NCS-treated cells overexpressing these five different USPs. As shown in Figure 3C, FK2-positive foci were readily detected in cells expressing NLS-GFP, NLS-USP46-GFP/UAF1, YFP-USP7 or YFP-USP22. In line with a previous report [49], a diffuse FK2 staining, but no NCS-induced foci, was observed in cells expressing YFP-USP3. As described above, FK2 signal was virtually undetectable in cells expressing of USP1/UAF1.

This article is protected by copyright. All rights reserved

Author Manuscript

In summary, these findings suggest that, when expressed at similar levels, the USP1/UAF1 complex exhibits comparatively higher substrate promiscuity than other nuclear DUBs in a cellular context.

ML323 reverts the effect of USP1/UAF1 overexpression on nuclear ubiquitin conjugation and 53BP1 recruitment

The drastic reduction in nuclear ubiquitin conjugation and the blockade of 53BP1 recruitment into foci in cells overexpressing USP1/UAF1 provide two clear-cut readouts for the activity of the complex in intact cells. These readouts could be the basis for a novel immunofluorescence-based approach to identify inhibitors of USP1/UAF1 function. As a proof-of-concept experiment, we sought to evaluate the cellular activity of ML323 using these readouts. To this end, cells co-transfected with GFP-USP1 and Xpress-UAF1 were pre-treated with ML323 for 2 hours, and NCS was then added for an additional 2 hours. As shown in Figure 4, both the depletion of conjugated ubiquitin (Figure 4A), and the blockade of 53BP1 recruitment (Figure 4B) in cells overexpressing the complex, were clearly reverted by ML323, further confirming the ability of ML323 to block USP1/UAF1 activity in cells.

Functional characterization of experimental mutations in USP1 Fingers subdomain.

The novel readouts for USP1/UAF1 activity described here can also be useful as experimental tools to shed further light on how the formation and function of the complex is regulated. In this regard, although USP1 deubiquitinase activity is crucially dependent on UAF1 interaction [7], and this interaction is mediated by USP1 Fingers subdomain [26], the specific USP1 residues that contribute to UAF1 binding remain to be mapped, and the potential effect of Fingers subdomain mutations on the activity of the USP1/UAF1 complex has not been investigated. To address these issues, we used depletion of conjugated ubiquitin and blockade of 53BP1 foci, along with other functional readouts summarized in Table 1, to characterize in detail a series of experimental and naturally-occurring USP1 Fingers mutants.

First, we used ClustalW2-based sequence alignment to compare the Fingers of USP1 with the Fingers of USP46, an amino acid segment that also binds UAF1 [26] and the Fingers of USP7, a segment that does not bind UAF1, (data not shown). Since the front of the Fingers subdomain represents the primary site for ubiquitin binding in most USP-family DUBs [21,22,23], we reasoned that residues at the back of the Fingers would be more likely to be involved in USP1/UAF1 interaction. As illustrated in Figure 5A, we selected four USP1 residues (R439, L441, L446 and S494) that are relatively well conserved in USP46, but not in USP7, and would be exposed at the back of the Fingers subdomain in a hypothetical three-dimensional model of USP1 based on the solved structure of USP7 [21]. We generated a mutant, termed GFP-USP1^{4m}, in which these four amino acids were replaced with the corresponding USP7 residues (R439Q/L441K/L446R/S494A). In addition to USP1^{4m}, three other USP1 mutants, USP1^{VE}, USP1^{IV} and USP1$^{VE/IV}$ (Figure 5B) bearing different alanine substitutions in a short sequence

This article is protected by copyright. All rights reserved

Author Manuscript

motif (^{495}VERIV) that resembles an essential UAF1 binding site in the HPV11 E1 helicase [50] were also tested.

We have reported before that UAF1 binding is not disrupted by mutation of USP1 ^{495}VERIV motif [51]. Here, using a previously described nuclear relocation assay [51], we found that GFP-USP1^{4m} is also able to bind UAF1 (Figure 6A). As a negative control, a deletion mutant lacking the Fingers subdomain, YFP-USP1del(420-520), did not induce UAF1 relocation to the nucleus. On the other hand, we evaluated the ability of USP1 Finger mutants to undego autocleavage at the 670GG diglycine motif, which represents a well-known mechanism that regulates USP1 function [10], and can be experimentally induced by co-expression with UAF1 [26]. UAF1 co-expression resulted in autocleavage of wild type USP1 and the Finger mutants (Figure 6B), whereas a catalytically inactive mutant (USP1^{C90S}), included as a negative control, did not undergo autocleavage when co-expressed with UAF1. Regarding cellular activity, GFP-USP1^{VE} retained the ability of wild type USP1 to deplete conjugated ubiquitin and block 53BP1 relocation to DNA damage foci (Figure 6C, D). In contrast, FK2 staining and 53BP1 foci were readily detected in cells overexpressing GFP-USP1^{IV}, GFP-USP1$^{VE/IV}$ and GFP-USP1^{4m}. To further substantiate these findings, we tested the ability of the mutants to revert hydroxyurea (HU)-induced monoubiquitination of PCNA, a well-established physiological substrate of the USP1/UAF1 complex. As shown in Figure 6E, expression of wild type GFP-USP1 or the mutant GFP-USP1^{VE} reduced the levels of monoubiquitinated PCNA (ubPCNA) in HU-treated cells. In contrast, ubPCNA levels in cells expressing GFP-USP1^{IV}, GFP-USP1$^{VE/IV}$ and GFP-USP1^{4m} were similar to those of cells expressing the empty vector or the catalytically inactive GFP-USP1^{C90S}.

Altogether, our data indicate that mutations in USP1 Fingers may severely impair the ability of the USP1/UAF1 complex to deubiquitinate cellular substrates without disrupting the complex or interfering with USP1 autocleavage.

Functional characterization of cancer-related mutations in USP1 Fingers subdomain

In order to extend our functional analysis to naturally-occurring USP1 mutations, we selected two missense mutations in Fingers domain residues (S475Y and D502N), which have been detected in endometrial carcinoma and melanoma samples, respectively (**http://cancer.sanger.ac.uk/cancergenome/projects/cosmic/**), and a third mutation, S575R, which is located outside the Fingers but affects the most commonly mutated USP1 residue in tumors. GFP-USP1^{S475Y}, GFP-USP1^{D502N} and GFP-USP1^{S575R} were able to promote the nuclear relocation of UAF1 (Figure 7A) and undergo UAF1-promoted autocleavage (Figure 7B). Subsequent cellular activity assays revealed that the S475Y mutation, but not the other two cancer-related mutations tested, abrogates USP1 ability to deplete conjugated ubiquitin (Figure 7C), prevent 53BP1 recruitment to DNA damage foci (Figure 7D) and reduce ubPCNA levels in

This article is protected by copyright. All rights reserved

Author Manuscript

cells treated with HU (Figure 7E) or with the DSB-inducer methyl methanesulfonate (MMS) (Figure 7F).

DISCUSSION

The role of the USP1/UAF1 deubiquitinase complex as an important regulator of DNA repair has been firmly established. Besides its well-known functions as a key regulator the Fanconi anemia (FA) pathway [9] and translesion synthesis (TLS) [10], several observations have been reported that, altogether, suggest a potentially broader role of the USP1/UAF1 complex in the cellular response to DNA damage [11,12,13]. To further explore this possibility, we tested the effect of modulating the function of the USP1/UAF1 complex on general protein ubiquitination, as well as on the levels and localization of two proteins involved in the response to DNA double strand breaks (DSBs), γH2AX and 53BP1.

Interfering with USP1/UAF1 activity increased the recruitment of ubiquitinated proteins into discrete nuclear foci, albeit not as dramatically as treatment with the DSB-inducing agent NCS. In line with the results of previous siRNA screenings [40,42], we found that USP1 knockdown has an effect on the levels of γH2AX. Of note, USP1 silencing seems to increase γH2AX levels in cells not exposed to DNA damage [40, and the present report), but to decrease γH2AX levels in cisplatin-treated cells [42]. Although these seemingly contradictory findings will require further clarification, three independent studies, including ours, point to a role for USP1 modulating the level of H2AX phosphorylation, a key apical event in the response to DSBs. Downstream of γH2AX in the DSB repair pathway, we found that interfering with USP1/UAF1 function increased the number of 53BP1 foci in the nuclei of 293T cells not exposed to genotoxic stress, which is consistent with the results of a previous study [52]. We noted that ML323 treatment resulted in a more pronounced increase in the number of FK2 or 53BP1 foci than USP1 knockdown. This observation may reflect a more complete blockade of USP1/UAF1 function by ML323, or suggest that the drug has additional effects besides inhibiting USP1/UAF1. Altogether, the results of our siRNA-based or inhibitor-based experiments support previously reported evidence [11,12,13] suggesting a potentially broader role of USP1/UAF1 in the response to DNA damage beyond its functions in FA and TLS.

In an attempt to gauge to what extent the observed effects are a direct consequence of USP1/UAF1 activity, we increased the cellular levels of the complex by co-transfecting GFP-USP1 and Xpress-UAF1. Two previous DUB overexpression screenings have reported that USP1, when expressed alone, does not block 53BP1 recruitment to DNA damage foci [46,48]. Strikingly, USP1/UAF1 overexpression (but not overexpression of USP1 alone) resulted in a drastic reduction of conjugated ubiquitin in the nucleus, as determined by FK2 immunostaining. In a comparison with other USPs, general ubiquitin deconjugation was not observed in the

This article is protected by copyright. All rights reserved

Author Manuscript

nucleus of cells expressing USP3, USP22 or NLS-USP46, and was only noted in cells expressing medium to high levels of USP7. Thus USP1/UAF1 behaves as a relatively more promiscuous deubiquitinase, when overexpressed in cells. It is presently unclear if this apparent promiscuity reflects non-specific substrate deubiquitination or indicates that USP1 has a larger repertoire of specific nuclear substrates than other DUBs. Of note, USP1/UAF1 and USP7 have been shown to exhibit relatively higher enzymatic activity when compared to other USPs using biochemical analyses with artificial substrates [7,44,53,54]. Our data suggest that this relatively higher enzymatic activity *in vitro* translates into a comparatively higher substrate promiscuity of these USPs when ectopically expressed in cells. Such promiscuity limits the usefulness of USP1/UAF1 overexpression experiments to explore the role of the complex in specific cellular pathways and to identify its physiological substrates. Admittedly, in the context of our study, it is not possible to establish to what extent general ubiquitin deconjugation contributes to the observed blockade of 53BP1 recruitment to DSB foci in cells overexpressing USP1/UAF1. More generally, although the number of DUBs compared in our study is certainly limited, our findings suggest that potential promiscuity should be taken into account when interpreting the results of DUB overexpression screenings.

From a practical point of view, general ubiquitin deconjugation and blockade of 53BP1 foci recruitment represent two clear-cut readouts for USP1/UAF1 activity in cells, which could be easily evaluated using automated microscopy. Using these readouts we have further confirmed the ability of ML323 to inhibit USP1/UAF1 activity, providing proof-of-concept evidence that they could be the basis for an immunofluorescence-based assay to identify novel USP1/UAF1 inhibitors. Furthermore, these novel readouts expand the battery of tests that can be used in structure-function studies to interrogate the effect of mutations in different domains of USP1. Here, we have focused on the Fingers subdomain, a segment that mediates UAF1 interaction [26] and that, by analogy to other USPs [21,22,23], would also be involved ubiquitin binding. Interestingly, our data show that certain experimental mutations in the Fingers subdomain, while preserving the ability of USP1 to bind to and be activated by UAF1 (as determined by its ability to undergo autocleavage), abrogate the ability of the USP1/UAF1 complex to promote substrate deubiquitination**.** In our view, there are at least two reasonable explanations for these findings. On one hand, it is possible that Finger mutations interfere with the binding of the ubiquitin moiety in substrates to the complex. An alternative possibility is that the catalytic activity of USP1 is affected by these mutations in such a manner that cleavage of ubiquitin moieties is perturbed, but the ability to cleave the peptide bond at the 670GG motif in the USP1 molecule is retained. More importantly, since there is still limited knowledge on the effect that cancer-related missense mutations may have on DUB function, we extended this analysis to naturally occurring USP1 Fingers mutations that have been detected in tumor samples. Previously, we have identified a cancer mutation (L699P) that hampers USP1 autocleavage

This article is protected by copyright. All rights reserved

Author Manuscript

[26]. Here, we identify a single aminoacid change in the Fingers subdomain (S475Y) that abrogates substrate deubiquitination without impairing UAF1 binding or autocleavage. Cancer-related missense mutations that result in decreased deubiquitination activity have been identified in other DUBs, including USP7 [55]. However, to the best of our knowledge the S575Y substitution is the first cancer-related loss-of function missense mutation identified in USP1.

MATERIALS AND METHODS

Plasmids, cloning procedures, siRNAs and site-directed mutagenesis

The plasmid encoding wild type GFP-USP1 was kindly provided by René Bernards (Netherlands Cancer Institute, Amsterdam). Plasmids containing the full-length cDNA of USP3 and USP7 were provided by Pier Paolo Di Fiore (University of Milan) and Roger Everett (University of Glasgow), respectively. A plasmid encoding Flag-HA-USP22 was provided by John W. Harper (Harvard Medical School, Boston) through Addgene (#22575). Finally, the plasmid encoding, Xpress-UAF1 was provided by Jae U. Jung (University of Southern California, Los Angeles). The plasmids encoding YFP-USP3 and YFP-USP7, NLS-USP46-GFP, YFP-USP1Del(420-520), GFP-USP1^{C90S} and UAF1-mRFP were generated as previously described [26,51,56]. To generate the plasmid encoding YFP-USP22, USP22 cDNA was amplified by PCR using high fidelity Pfu UltraII fusion HS DNA polymerase (Stratagene), and subcloned into pEYFP-C1 (Clontech) as a KpnI/BamHI fragment.

A pool of three siRNAs (Ambion, Life Technologies) targeting USP1 (s14723, s14724, s14725) and a pool of two siRNAs targeting USP11 (s15739, s15740) were used in knockdown experiments. Scramble siRNA silencer select siRNA #1 was used as a negative control.

USP1 mutations were introduced using the Quick-Change Lightning Site-Directed Mutagenesis Kit (Stratagene), according to manufacturer's directions. All the new constructs generated were subjected to DNA sequencing (Stabvida), and the absence of any unwanted mutation was confirmed. The sequences of the oligonucleotides used in cloning and site-directed mutagenesis are available upon request.

Cell culture, transfections and drug treatments

Human embryonic kidney 293T (HEK293T) cells were grown in Dulbecco's modified Eagle's medium, supplemented with 10% fetal bovine serum, 100 U/ml penicillin and 100 μg/ml streptomycin (all from Invitrogen). Twenty four hours before transfection, cells were seeded onto 12-well or 6-well tissue culture plates. Plasmid transfections were carried out using X-tremeGENE 9 transfection reagent (Roche Diagnostics) following manufacturer's protocol. siRNA transfections were carried out using Lipofectamine RNAiMAX (Invitrogen). 10 nM siRNA was used per sample.

Cells were treated with the following drugs: ML323 (Calbiochem) at 50μM for 4 or 16h, neocarzinostatin (NCS, Sigma-Aldrich) at 100mg/ml for 2 or 4h, hydroxyurea (HU, Sigma-

This article is protected by copyright. All rights reserved

Author Manuscript

Aldrich) at 4mM for 24 h and Methyl methanesulfonate (MMS, Sigma-Aldrich) at 1mM for 1h. MMS treatment was followed by a 3 h recovery in drug-free medium.

Immunofluorescence, confocal microscopy and image analysis

Cells, growing onto sterile coverslips, were fixed with 3,7% formaldehyde in phosphate-buffered saline (PBS) for 30 min, permeabilized with 0,2% Triton X-100 in PBS for 10 min, blocked for 1h in blocking solution (3% BSA in PBS) and incubated with primary antibodies diluted in blocking solution for 1h at room temperature. The following primary antibodies and dilutions were used: FK2 (Enzo, 1:500), γH2AX-Ser319 (Millipore, 1:500), 53BP1 (Novus, 1:200), H3K56Ac (Abcam, 1:200), H3K4Me3 (Abcam, 1:200) and H3K9Me3 (Cell Signaling Technology, 1:100). Cells were next washed with PBS and incubated with secondary antibodies (Alexa Fluor 488 anti-mouse and Alexa Fluor 594 anti-mouse/rabbit; Invitrogen, 1:400) for 1h at room temperature. Coverslips were washed with PBS and mounted onto microscope slides using Vectashield mounting medium with DAPI (Vector Laboratories). Samples were analyzed using an Olympus Fluoview FV500 confocal microscope equipped with FV-viewer software. To avoid bias in the quantitation of FK2 and 53BP1 foci, slides were coded, and images were taken and examined by an observer unaware of the identity of the samples.

Image analysis with ImageJ software was used to quantify the intensity of the FK2 or γH2AX immunoflorescence signal, as well as the intensity of GFP/YFP fluorescence.

The number of cells examined in each experiment is indicated in the corresponding Figure legend.

Immunoblot analysis

Cells were washed with ice-cold PBS and collected in lysis buffer containing 10 mM sodium phosphate (pH 7.4), 150 mM NaCl, 1 mM EDTA, 1 mM EGTA, 10 mM β-glycerophosphate, 0.5% NP40, 10 mM phenylmethylsulfonylfluoride, 10 mM sodium orthovanadate, 10 μg/ml protease inhibitor cocktail (Roche), and 50 mM N-ethylmaleimide (Thermo Scientific). Protein concentration was determined using the DC Protein Assay (Bio-Rad). Protein samples were separated in 12% or 8% SDS-PAGE and transferred onto a nitrocellulose membrane (Bio-Rad). Prior to antibody incubation, membranes were stained with Ponceau to assess protein loading. Membranes were blocked with 5% non-fat dry milk in TTBS and blotted with primary antibodies. The following primary antibodies and dilutions were used: anti-Xpress (Invitrogen, 1:5000), anti-PCNA (Santa Cruz 1:400), anti-GFP (Chromotek, 1:1000), anti-β-actin (Sigma-Aldrich, 1:3000) and anti-α-tubulin (Sigma-Aldrich, 1:5000). Subsequently, membranes were incubated with the corresponding horseradish peroxidase-conjugated secondary antibodies (Santa cruz, 1:3000), and developed with ECL reagent (Thermo Scientific). Semiquantitave analysis of immunoblot bands was performed by densitometry using Quantity One software 4.6 (Bio-Rad Laboratories).

Statistical analysis

This article is protected by copyright. All rights reserved

Author Manuscript

Statistical calculations were performed with Graphpad Prism Software (Graphpad, San Diego, CA, USA). All analyses are two-tailed Student´s t-test and error bars represent standard-error of the mean (SEM).

ACKNOWLEDGEMENTS

We appreciate the generous gift of plasmids from Dr. René Bernards (Netherlands Cancer Institute), Pier Paolo Di Fiore (University of Milan), Dr. Roger Everett (University of Glasgow), Dr. Jae Jung (University of Southern California) and Dr. John W. Harper (Harvard Medical School). We appreciate the technical support by the staff from the High Resolution Microscopy Facility (SGIKER-UPV/EHU). We are very grateful to Dr. Sonia Bañuelos (Dept. of Biochemistry and Molecular Biology, UPV/EHU) for helpful discussions and for preparing the USP1 models. This work was supported by the Basque Country Government Department of Industry (grant number ETORTEK BioGUNE2010 to JAR), the Spanish Government MICINN (Ministerio de Ciencia e Innovacion) (grant number BFU2009-13,245 to JAR), the University of the Basque Country (UFI11/20), fellowships from the Department of Education of the Basque Country Government and the UPV/EHU (to IG-S), and a fellowship from the University of the Basque Country (to AO-H). This article is based upon work from COST Action (PROTEOSTASIS BM1307), supported by COST (European Cooperation in Science and Technology).

AUTHOR CONTRIBUTIONS

AO-H, IG-S and JAR planned and performed experiments, and analyzed the data; AO-H and JAR wrote the paper.

REFERENCES

1. Jackson SP & Bartek J (2009) The DNA-damage response in human biology and disease. *Nature* **461**,1071-1078.

2. Lukas J, Lukas C & Bartek J (2004) Mammalian cell cycle checkpoints: _ignaling pathways and their organization in space and time. *DNA Repair (Amst)* **3**, 997-1007.

3. Zhao Y, Brickner JR., Majid MC & Mosammaparast N (2014) Crosstalk between ubiquitin and other post-translational modifications on chromatin during double-strand break repair. *Trends. Cell Biol* **24**, 426-434.

4. Ulrich HD &Walden H (2010) Ubiquitin _ignaling in DNA replication and repair. *Nat. Rev. Mol. Cell Biol* **11**, 479-489.

This article is protected by copyright. All rights reserved

Author Manuscript

5. Komander D & Rape M (2012) The ubiquitin code. *Annu. Rev. Biochem* **81**, 203–229.

6. Jacq X, Kemp M, Martin NMB & Jackson SP (2013) Deubiquitylating enzymes and DNA Damage Response pathways. *Cell Biochem. Biophys* **67**, 25-43.

7. Cohn MA, Kowal P, Yang K, Haas W, Huang TT, Gygi SP & D´Andrea AD (2007) A UAF1 containing multisubunit protein complex regulates the Fanconi anemia pathway. *Mol. Cell* **28**, 786-797.

8. Cohn MA, Kee Y, Hass W, Gygi SP & D´Andrea AD (2009) UAF1 is a subunit of multiple deubiquitinating enzyme complexes. *J. Biol. Chem* **284**, 5343-5351.

9. Nijman SM, Huang TT, Dirac AM, Brummelkamp TR, Kerkhoven RM, D´Andrea AD & Bernards R (2005) The deubiquitinating enzyme USP1 regulates the Fanconi anemia pathway. *Mol. Cell* **17**, 331-339.

10. Huang TT, Nijman SM, Mirchandani KD, Galardy PJ, Cohn MA, Haas W, Gygi SP, Ploegh HL, Bernards R & D´Andrea AD (2006) Regulation of monoubiquitinated PCNA by DUB autocleavage. *Nat. Cell. Biol* **8**, 339-347.

11. Kim JM, Parmar K, Huang M, Weinstock DM, Ruit CA, Kutok JL & D´Andrea AD (2009) Inactivation of murine usp1 results in genomic instability and fanconi anemia phenotype. *Dev. Cell* **16**, 314-320.

12. Murai J, Yang K, Dejsuphong D, Hirota K, Takeda S & D´Andrea A.D (2011) The USP1/UAF1 complex promotes double-strand break repair through homologous recombination. *Mol. Cell Biol* **31**, 2462-2469.

13. Nishi R, Wijnhoven P, Le Sage C, Tjeertes J, Galanty Y, Forment JV, Clage MJ, Urbé S & Jackson SP (2014) Systematic characterization of deubiquitylating enzymes for roles in maintaining genome integrity. *Nat. Cell Bio*l **16**,1016-1026.

14. Williams SA, Maecker HL, French DM, Liu J, Gregg A, Silverstein LB, Cao TC, Carano RA & Dixit VM (2011) USP1 deubiquitinates ID proteins to preserve a mesenchymal stem cell program in osteosarcoma. *Cell* **146**, 918-930.

15. García-Santisteban I, Peters GJ, Giovannetti E & Rodriguez JA (2013) USP1 deubiquitinase: cellular functions, regulatory mechanisms and emerging potential as target in cancer therapy. *Mol. Cancer* **12**, 91.

This article is protected by copyright. All rights reserved

Author Manuscript

16. Oestegard VH, Langevin F, Kuiken HJ, Pace P, Niedzwiedz W, Simspon LJ, Ohzeki M, Takata M, Sale JE & Patel KJ (2007) Deubiquitination of FANCDS is required for DNA crosslink repair. *Mol. Cell* **28**, 798-809.

17. Chen J, Dexheimer TS, Ai Y, Liang Q, Villamil MA, Inglese J, Maloney DJ, Jadhav A, Simeonov A & Zhuang Z (2011) Selective and cell active inhibitors of the USP1/UAF1 deubiquitinase complex reverse cisplatin resistance in non-small cell lung cancer cells. *Chem. Biol* **18**, 1390-1400.

18. Mistry H, Hsieh G, Buhrlage SJ, Huang M, Park E, Cuny GD, Galinsky I, Stone RM, Gray NS, D´Andrea AD & Parmar K (2013) Small-molecule inhibitors of USP1 target ID1 degradation in leukemic cells. *Mol Cancer Ther* **12**, 2651–2662.

19. Liang Q, Dexheimer TS, Zhang P, Rosenthal AS, Villamil MA, You C, Zhang Q, Chen J, Ott CA, Sun H, Luci DK, Yuan B, Simeonov A, Jadhav A, Xiao H, Wang Y, Maloney DJ & Zhuang Z (2014) A selective USP1-UAF1 inhibitor links deubiquitination to DNA damage responses. *Nat. Chem. Biol* **10**, 298-304.

20. Dexheimer TS, Rosenthal AS, Luci DK, Liang Q, Villamil MA, Chen J, Sun H, Kerns EH, Simeonov A, Jadhav A, Zhuang Z & Maloney DJ (2014) Synthesis and structure-activity relationship studies of N-benzyl-2-2phenylpyrimidin-4-amine derivates as potent USP1/UAF1 deubiquitinase inhibitors with anticancer activity against nonsmall cell lung cancer. *J. Med. Chem* **57**, 8099-8110.

21. Hu M, Li P, Li M, Li W, Yao T, Wu JW, Gu W, Cohen RE & Shi Y (2002) Crystal structure of a UBP-family deubiquitinating enzyme in isolation and in complex with ubiquitin aldehyde. *Cell* **111**, 1041–1054.

22. Hu M, Li P, Song L, Jeffrey PD, Chenova TA, Wilkinson KD, Cohen RE & Shi Y (2005) Structure and mechanisms of the proteasome-associated deubiquitinating enzyme USP14. *EMBO J* **2**, 3747–3756.

23. Renatus M, Parrado SG, D'Arcy A, Eidhoff U, Gerhartz B, Hassiepen U, Pierrat B, Riedl R, Vinzen D, Worpenberg S & Kroemer M (2006) Structural basis of ubiquitin recognition by the deubiquitinating protease USP2. *Structure* **14**, 1293–1302.

24. Ye Y, Scheel H, Hofmann K & Komander D (2009) Dissection of USP catalytic domains reveals five common insertion points. *Mol Biosyst* **5**, 1797–1808.

25. Komander D, Clague MJ & Urbé S (2009) Breaking the chains: structure and function of the deubiquitinases. *Nat Rev Mol Cell Biol* **10**, 550–563.

This article is protected by copyright. All rights reserved

Author Manuscript

26. Olazabal-Herrero A, García-Santisteban I & Rodríguez JA (2015) Structure-function analysis of USP1: insights into the role of Ser313 phosphorylation site and the effect of cancer-associated mutations on autocleavage. *Mol. Cancer* **14**,33.

27. Fujimuro M, Sawada H & Yokosawa H (1994) Production and characterization of monoclonal antibodies specific to multi-ubiquitin chains of polyubiquitinated proteins. *FEBS Lett* **349**, 173-180.

28. Messick TE & Greenberg RA (2009) The ubiquitin landscape at DNA double-strand breaks. *J. Cell Biol* **187**, 319-326.

29. Bencokova Z, Kaufmann MR, Pires IM, Lecane PS, Giaccia AJ & Hammond EM (2009) ATM activation and signaling under hypoxic conditions. *Mol. Cell Bio*l **29**, 526-537.

30. Morris C, Tomimatsu N, Richard DJ, Cluet D, Burma S, Khanna KK & Jalinot P (2012) INT6/EIF3E interacts with ATM and is required for proper execution of the DNA damage response in human cells. *Cancer Res* **72**, 2006-2016.

31. van Wijk SJ, Fiskin E, Putyrski M, Pampaloni F, Hou J, Wild P, Kensche T, Grecco HE, Bastiaens P & Dikic I (2012) Fluorescence-based sensors to monitor localization and functions of linear and K63-linked ubiquitin chains in cells. *Mol. Cell* **47**, 797-809.

32. Kato K, Nakajima K, Ui A, Muto-Terao Y, Ogiwara H & Nakada S (2014) Fine-Tuning of DNA Damage-Dependent Ubiquitination by OTUB2 Supports the DNA Repair Pathway Choice. *Mol. Cell* **53**, 617-630.

33. Fernandez-Capetillo O, Lee A, Nussenzweig M & Nussenzweig A (2004) H2AX: the histone guardian of the genome. *DNA Repair (Amst.)* **3**, 959-967.

34. Rogakou EP, Pilch D., Orr AH, Ivanova VS & Bonner WM (1998) DNA double-stranded breaks induce histone H2AX phosphorylation on serine 139. *J. Biol. Chem* **273**, 5858-5868.

35. Stucki M, Clapperton JA, Mohammad D, Yaffe MB, Smerdon SJ & Jackson SP (2005) MDC1 directly binds phosphorylated histone H2AX to regulate cellular responses to DNA double-strand breaks. Cell **123**, 1213-1226.

36. Huen MS, Grant R, Manke I, Minn K, Yu X, Yaffe MB & Chen J (2007) RNF8 transduces the DNA-damage signal via histone ubiquitylation and checkpoint protein assembly. *Cell* **131**, 901-914.

This article is protected by copyright. All rights reserved

Author Manuscript

37. Mailand N, Bekker-Jensen S, Faustrup H, Melander F, Bartek J, Lukas C & Lukas J (2007) RNF8 ubiquitylates hiestones at DNA double-strand breaks and promotes assembly of repair proteins. *Cell* **131**, 887-900.

38. Doil C, Mailand N, Bekker-Jensen S, Menard P, Larsen DH, Pepperkok R, Ellenberg J, Panier S, Durocher D, Bartek J, Lukas J & Lukas C (2008) RNF168 binds and amplifies ubiquitin conjugates on damaged chromosomes to allow accumulation of repair proteins. *Cell* **136**, 435-446.

39. Huyen Y, Zgheib O, Ditullio RA Jr, Gorgoulis VG, Zacharatos P, Petty TJ, Sheston EA, Mellert HS, Stavridi ES & Halazonetis TD (2004) Methylated lysine 79 of histone H3 targets 53BP1 to DNA double-strand breaks. *Nature* **432**, 406-411.

40. Lovejoy CA, Xu X, Bansbach CE, Glick GG, Zhao R, Ye F, Sirbu BM, Titus LC, Shyr Y & Cortez D (2009) Functional genomic screens identify CINP as a genome maintenance. *Proc. Natl. Acad. Sci* **106**, 19304-19309.

41. Luijsterburg MS & van Attikum H (2011) Chromatin and the DNA damage response: The cancer connection. *Mol. Oncol* **5**, 349-367.

42. Schmidt F, Kunze M, Loock A & Dobbelstein M (2015) Screening analysis of ubiquitin ligases reveals G2E3 as a potential target for chemosensitizing cancer cells. *Oncotarget* **6**, 617-632.

43. Wiltshire TD, Lovejoy CA, Wang T, Xia F, O´Connon MJ & Cortez D (2010) Sensitivity to Poly(ADP-ribose) Polymerase (PARP) inhibition identifies Ubiquitin-Specific Peptidase 11 (USP11) as a regulator of DNA double-strand break repair. *J. Biol. Chem* **285**, 14565-14571.

44. Faesen AC, Luna-Vargas MP, Geurink PP, Clerici M, Merkx R, van Dijk WJ, Hameed DS, El Oualid F, Ovaa H & Sixma TK (2011) The differential modulation of USP activity by internal regulatory domains, interactors and eight ubiquitin chain types. *Chem Biol* **18**, 1550–1561.

45. Endo A, Matsumoto M, Inada T, Yamamoto A, Nakayama KI, Kitamura N & Komada M (2009) Nucleolar structure and function are regulated by the deubiquitylating enzyme USP36. *J Cell Sci*. **122**, 678-686.

46. Mosbech A, Lukas C, Bekker-jensen S & Mailand N (2013) The deubiquitinating enzyme USP44 counteracts the DNA double-strand break response mediated by the RNF8 and RNF168 ubiquitin ligases. *J. Biol. Chem* **288**, 16579-16587.

This article is protected by copyright. All rights reserved

Author Manuscript

47. Zhang Z, Yang H & Wang H (2014) The histone H2A deubiquitinase USP16 interacts with HERC2 and fine-tunes cellular response to DNA damage. *J. Biol. Chem* **289**, 32883-32894.

48. Typas D, Luijsterburg MS, Wiegant WW, Diakatou M, Helfricht A, Thijssen PE, van de Broek B, Mullenders LH & van Attikum H (2015) The de-ubiquitylating enzymes USP26 and USP37 regulate homologous recombination by counteracting RAP80. *Nucleic Acid Res* **43**, 6919-6933.

49. Sharma N, Zhu Q, Wani G, He J, Wang Q & Wani AA (2014) USP3 counteracts RNF168 via deubiquitinating H2A and γH2AX at lysine 13 and 15. *Cell Cycle* **13**, 106-114.

50. Côté-Martin A, Moody C, Fradet-Turcotte A, D'Abramo CM, Lehoux M, Joubert S, Poirier GG, Coulombe B, Laimins LA & Archambault J (2008) Human papillomavirus E1 helicase interacts with the WD repeat protein p80 to promote maintenance of the viral genome in keratinocytes. *J. Virol* **82**, 1271-1283.

51. Garcia-Santisteban I, Zorroza K & Rodriguez JA (2012) Two nuclear localization signals in USP1 mediate nuclear import of the USP1/UAF1 complex. *PloS One* **7** doi: 10.1371/journal.pone.0038570.

52. Jones MJ, Colnaghi L & Huang TT (2012) Dysregulation of DNA polymerase κ recruitment to replication forks results in genomic instability. *EMBO* J **31**, 908-918.

53. Villamil MA, Chen J, Liang Q & Zhuang Z (2012) A noncanonical cysteine protease USP1 is activated through active site modulation by USP1-associated factor 1. *Biochemistry* **51**, 2829-2839.

54. Lee JG, Baek K, Soetandyo N & Ye Y (2013) Reversible inactivation of deubiquitinases by reactive oxygen species in vitro and in cells. *Nat Commun* **4**, 1568.

55. Huether R, Dong L, Chen X, Wu G, Parker M, Wei L, Ma J, Edmonson MN, Hedlund EK, Rusch MC, Shurtleff SA, Mulder HL, Boggs K, Vadordaria B, Cheng J, Yergeau D, Song G, Becksfort J, Lemmon G, Weber C, Cai Z, Dang J, Walsh M, Gedman AL, Faber Z, Easton J, Gruber T, Kriwacki RW, Partridge JF, Ding L, Wilson RK, Mardis ER, Mullighan CG, Gilbertson RJ, Baker SJ, Zambetti G, Ellison DW, Zhang J & Downing JR (2014) The landscape of somatic mutations in epigenetic regulators across 1,000 paediatric cancer genomes. *Nat Commun* **5**, 3630.

56. García-Santisteban I, Bañuelos S & Rodríguez JA (2012) A global survey of CRM1-dependent nuclear export sequences in the human deubiquitinase family. *Biochem J* **441**, 209-217.

This article is protected by copyright. All rights reserved

Author Manuscript

SUPPORTING INFORMATION

Figure S1: Efficacy of siRNA-mediated knockdown of USP1 and USP11.

Author Manuscript

FIGURE LEGENDS

Figure 1. Effect of modulating USP1/UAF1 function on general ubiquitin conjugation in the nucleus.

A. Immunoblot shows efficacy of USP1 silencing in 293T cells using a pool of three siRNAs targeting USP1 (siUSP1). A scramble siRNA was used as negative control (siCTRL). Confocal microscopy images show representative examples of FK2 immunostaining in 293T cells transfected with a control siRNA or with USP1-targeting siRNAs. DAPI was used to counterstain the nucleus (DNA panels). Graph represents the percentage of cells showing more than five FK2-positive nuclear foci in each condition. B. Confocal microscopy images of FK2 immunostaining in 293T cells untreated (UT) or treated with the USP1/UAF1 inhibitor ML323 (50μM) for 16h. Graph represents the percentage of cells showing more than five FK2-positive nuclear foci in each condition. In panels A and B, the data shown in the graphs correspond to the mean of four independent experiments and error bars indicate the standard error of the mean (SEM). 100 cells per condition were examined in each experiment. *$p<0.05$; **$p<0.01$ (Student´s t-test). C. Confocal microscopy images of FK2 immunostaining in 293T cells transfected with expression plasmids encoding a NLS-GFP negative control (NLS), GFP-USP1 alone (USP1), GFP-USP1 wild type ($USP1^{WT}$) plus Xpress-UAF1, or a catalytically inactive GFP-USP1 mutant ($USP1^{C90S}$) plus Xpress-UAF1. The nucleus of a representative transfected cell in each sample is circled by a dotted line. The intensity of the FK2 immunofluorescence signal in the nucleus of at least 50 transfected cells with similar GFP expression levels per sample was quantified using Image J software. In the graph on the right, each dot represents the intensity of the FK2 signal in the nucleus of a single cell, and the bar indicates the median. The data shown correspond to one experiment. Two independent experiments were performed with similar results. D. Confocal microscopy images show FK2 immunostaining in 293T cells transfected as in panel C, and treated with 100mg/ml neocarzinostatin (+NCS) for 4h.

Figure 2. **Effect of modulating USP1/UAF1 function on γH2AX, H3K56Ac, H3K4Me3, H3K9Me3 and 53BP1.**

This article is protected by copyright. All rights reserved

A. Immunoblot shows efficacy of USP11 silencing in 293T cells using a pool of two siRNAs targeting USP11 (siUSP11). A scramble siRNA was used as negative control (siCTRL). The graph below represents the intensity of γH2AX immunofluorescence signal in the nucleus of 293T cells transfected with a control siRNA, or with siRNAs targeting USP11 and USP1. The intensity of the γH2AX signal in the nucleus of at least 100 cells per sample was quantified using Image J software. Each dot in the graph represents the intensity of the γH2AX signal in the nucleus of a single cell, and the bar indicates the median. The data shown correspond to one experiment. Two independent experiments were performed with similar results. On the right, confocal microscopy images showing examples of γH2AX immunostaining in 293T cells transfected with expression plasmids encoding YFP (vector) or co-transfected with plasmids encoding GFP-USP1 and Xpress-UAF1 (USP1/UAF1). Cells were treated with NCS (100mg/ml) for 4h to induce the recruitment of γH2AX into nuclear foci. B. On the left, confocal microscopy images showing representative examples of H3K56Ac immunostaining in 293T cells transfected with a control siRNA (siCTRL) or with a pool of three siRNAs tartegint USP1 (siUSP1). On the right, confocal microscopy images showing representative examples of H3K56Ac immunostaining in 293T cells transfected with expression plasmids enconding YFP (vector) or co-transfected with plasmids encoding GFP-USP1 and Xpress-UAF1 (USP1/UAF1) and treated with NCS (100mg/ml) for 4h. C, D. Confocal microscopy images showing representative examples of H3K4Me3 and H3K9Me3 staining in 293T transfected as in panel B. E. Confocal microscopy images showing representative examples of 53BP1 immunostaining in 293T cells transfected with a control siRNA (siCTRL) or with a pool of three siRNAs targeting USP1 (siUSP1). Graph represents the percentage of cells showing more than five 53BP1 nuclear foci in each condition. F. Confocal microscopy images of 53BP1 immunostaining in 293T cells untreated (UT) or treated with ML323 (50μM) for 16h. Graph represents the percentage of cells showing more than five 53BP1 nuclear foci in each condition. In panels E and F, the data shown in the graphs correspond to the mean of four independent experiments and error bars indicate the standard error of the mean (SEM). 100 cells per condition were examined in each experiment. ns= non-significant; **p<0.01 (Student´s t-test). G. Confocal microscopy images showing representative examples of 53BP1 immunostaining in 293T cells transfected with expression plasmids encoding a NLS-GFP negative control (NLS), GFP-USP1 alone (USP1), GFP-USP1 wild type ($USP1^{WT}$) and Xpress-UAF1, or a catalytically inactive GFP-USP1 mutant ($USP1^{C90S}$) and Xpress-UAF1. Cells were treated with NCS (100mg/ml) 4h before fixation. Graph represents the percentage of cells showing more than five 53BP1 nuclear foci in each sample. The data shown correspond to the mean of three independent experiments and error bars indicate the standard error of the mean (SEM). 100 cells per condition were examined in each experiment. **p<0.01 (Student´s t-test).

This article is protected by copyright. All rights reserved

Author Manuscript

Figure 3: Comparison of USP1/UAF1 with other nuclear USPs using depletion of conjugated ubiquitin as readout.

A. Confocal microscopy images show examples of FK2 immunostaining in 293T cells transfected with expression plasmids encoding a NLS-GFP negative control (NLS), GFP-USP1 plus Xpress-UAF1 (USP1/UAF1), NLS-USP46-GFP plus Xpress-UAF1 (USP46/UAF1), YFP-USP3, YFP-USP7 or YFP-USP22. B. Using Image J software, the intensity of the FK2 immunofluorescence and the YFP/GFP fluorescence in the nucleus of 50 cells per sample was quantified. FK2 intensity was normalized using the intensity of the signal in the nucleus of non-transfected cells, and then plotted against the YFP/GFP intensity. Each dot in the graph represents a single cell. Trend lines were added using Excel. The data shown correspond to one experiment. Three individual experiments were carried out, with similar results. C. Confocal microscopy images show examples of FK2 immunostaining in 293T cells transfected as in panel A, and treated with 100mg/ml neocarzinostatin (+NCS) for 4h.

Figure 4: ML323 reverts the effect of USP1/UAF1 overexpression on nuclear ubiquitin conjugation and 53BP1 recruitment.

A. Confocal microscopy images showing examples of FK2 immunostaining in 293T cells co-transfected with expression plasmids encoding GFP-USP1 and Xpress-UAF1. 24h after transfection, cells were either left untreated (upper set of panels) or treated with ML323 (50μM) for 2h (lower set of panels). NCS (100 mg/ml) was subsequently added, and samples were incubated for additional 2h before being fixed and immunostained. B. Confocal microscopy images show examples of 53BP1 immunostaining in 293T cells transfected and treated as in A.

Figure 5: Description of the experimental mutations introduced in USP1 Fingers subdomain.

A. ClustalW2-based sequence alignment of amino acid segments in the Fingers subdomains of USP1 (residues 420-520), USP46 (residues 165-259) and USP7 (residues 314-411). Letters are colored according to the physicochemical properties of the represented residue (**http://www.ebi.ac.uk/Tools/msa/clustalw2/help/faq.html**), and arrowheads indicate those residues whose properties are similar in USP1 and USP46, but different in USP7. Asterisks indicate the four cysteine residues that form a zinc-binding motif conserved in most USPs, including USP1 and USP46, but not in USP7 (24). Below, a model of USP1 catalytic domain based on homology with USP7 structure 1NB8 (21) is shown as a surface representation, depicted with Pymol program, and omitting the USP1 inserted domains not present in USP7. The structure of the USP catalytic domain resembles an “open right hand”, and both front and back views of the “hand” are shown. The Fingers sub-domain segment (residues 420-520) is colored cyan. Taking into account that Fingers subdomain sequences in USP1 and USP46, but not in USP7, mediate binding to UAF1 (26, and data not shown), and that the “front” side of the Fingers subdomain is involved in ubiquitin binding in USP-family DUBs (21-23), we

This article is protected by copyright. All rights reserved

Author Manuscript

hypothesized that some USP1 residues conserved in USP46 but not in USP7, and located on the "back" side of the Fingers might be particularly relevant for UAF1 binding and other specific functional properties of USP1 Fingers. Four USP1 residues that fulfill these requirements, R439, L441, L446 and S494 (indicated by black arrowheads in the alignment and highlighted in dark red in the model) were replaced with the corresponding USP7 residues to create the $USP1^{4m}$ mutant (R439Q/L441K/L446R/S494A). B. Amino acid sequence of USP1 segment 480-520 indicating the position of a VEIRV motif that resembles the essential UAF1 binding site in the HPV11 E1 helicase (50). Three different mutant versions of USP1 ($USP1^{VE}$, $USP1^{IV}$ and $USP1^{VE/IV}$), bearing the indicated alanine substitutions in this motif were tested.

Figure 6: Characterization of experimental mutations in USP1 Fingers subdomain.

A. Confocal microscopy images showing examples of 293T cells co-expressing UAF1-mRFP (red) and different GFP-USP1 constructs (green). B. Immunoblot analysis to test the ability of experimental USP1 Finger mutants to undergo UAF1-induced autocleavage. 293T cells were transfected with the indicated GFP-USP1 variants either alone (-) or in combination with Xpress-UAF1 (+). Anti-GFP antibody was used to detect GFP-USP1 and anti-Xpress antibody was used to detect Xpress-UAF1. α-tubulin was used as a loading control. The higher molecular weight band in the "USP1" blot corresponds to non-cleaved GFP-USP1, whereas the lower band corresponds to the N-terminal fragment that results from autocleavage at the 670GG motif. C. Confocal microscopy images showing examples of FK2 immunostaining in 293T cells co-transfected with expression plasmids encoding Xpress-UAF1 and either GFP-USP1 wild type (WT) or Finger subdomain mutant variants of GFP-USP1. Cells were treated with NCS (100mg/ml) 4h before being fixed and immunostained. D. Confocal microscopy images showing examples of 53BP1 immunostaining in 293T cells transfected and treated as in panel C. E. Immunoblot analysis of 293T cells co-transfected with Xpress-UAF1 and either empty YFP-vector, $GFP\text{-}USP1^{WT}$, the catalytically inactive mutant $USP1^{C90S}$ or the four USP1 Fingers subdomain mutants. Cells were either left untreated (UT) or treated with 4mM hydroxyurea for 24h. Using an anti-PCNA antibody, monoubiquitinated PCNA (ubPCNA) is detected as a band migrating slightly above the non-ubiquitinated form (PCNA). Anti-GFP and anti-Xpress antibodies were used to confirm expression of the transfected proteins. β-actin was used as a control for equal loading of the protein samples. The dotted line indicates that the panel is a composite of two images from a single exposure of the same gel. The ratio of ubiquitinated to non-ubiquitinated PCNA (ubPCNA/PCNA ratio) was determined by densitometry analysis of the immunoblot bands and normalized using the ubPCNA/PCNA ratio in cells expressing wild type GFP-USP1 as a reference. The graph on the right shows the results of this analysis. The data represent the mean and SEM of 3 independent experiments.

Figure 7: Characterization of cancer-related mutations in USP1 Fingers subdomain.

This article is protected by copyright. All rights reserved

Author Manuscript

A. Confocal images showing examples of 293T cells co-expressing UAF1-mRFP (red) and different GFP-USP1 constructs (green). B. Immunoblot analysis to test the ability of USP1 cancer-related mutants to undergo UAF1-induced autocleavage. 293T cells were transfected with the indicated GFP-USP1 variants either alone (-) or in combination with Xpress-UAF1 (+). Anti-GFP antibody was used to detect GFP-USP1 and anti-Xpress antibody was used to detect Xpress-UAF1. α-tubulin was used as a loading control. C. Confocal microscopy images showing examples of FK2 immunostaining in 293T cells co-transfected with expression plasmids encoding Xpress-UAF1 and either GFP-USP1 wild type (WT) or three different USP1 mutant variants that have been identified in tumor samples ($USP1^{S475Y}$, $USP1^{D502N}$ and $USP1^{S575R}$). Cells were treated with NCS (100mg/ml) 4h before fixation. The nucleus of a representative cell in each sample is circled by a dotted line. D. Confocal microscopy images showing examples of 53BP1 immunostaining in 293T cells transfected and treated as in panel C. E. Immunoblot analysis of 293T cells co-transfected with Xpress-UAF1 and either empty YFP-vector, $GFP\text{-}USP1^{WT}$, the catalytically inactive mutant $USP1^{C90S}$ or the three cancer-related USP1 mutants. Cells were either left untreated (UT) or treated with 4mM hydroxyurea for 24h. The non-ubiquitinated (PCNA) and monoubiquitinated (ubPCNA) forms of PCNA were detected using an anti-PCNA antibody. Anti-GFP and anti-Xpress antibodies were used to confirm expression of the transfected proteins. β-actin was used as a control for equal loading of the protein samples. The dotted line indicates that the panel is a composite of two images from a single exposure of the same gel. The ratio of ubiquitinated to non-ubiquitinated PCNA (ubPCNA/PCNA ratio) was determined by densitometry analysis of the immunoblot bands and normalized using the ubPCNA/PCNA ratio in cells expressing wild type GFP-USP1 as a reference. The graph on the right shows the results of this analysis. The data represent the mean and SEM of 3 independent experiments. F. Immunoblot analysis of 293T cells co-transfected as in panel E and either left untreated (UT) or treated with 1mM MMS for 1h, followed by a 3 h recovery in drug-free medium. The numbers below the ubPCNA bands indicate the ubPCNA/PCNA ratio.

Table 1. Results of the characterization of USP1 Fingers subdomain mutant variants using a battery of functional tests.

	TEST				
USP1 variant	UAF1 relocation	Autocleavage	FK2 depletion	Blockade of 53BP1 foci	PCNA deubiquitination
WT	+	+	+	+	+
C90S	+	-	-	-	-
Del (420-520)	-	n.t.*	n.t	n.t	n.t

This article is protected by copyright. All rights reserved

Author Manuscript

VE	+	+	+	+	+
IV	+	+	-	-	-
VE/IV	+	+	-	-	-
S475Y	+	+	-	-	-
D502N	+	+	+	+	+
S575R	+	+	+	+	+

*n.t.: not tested

Author Manuscript

This article is protected by copyright. All rights reserved

Figure 1

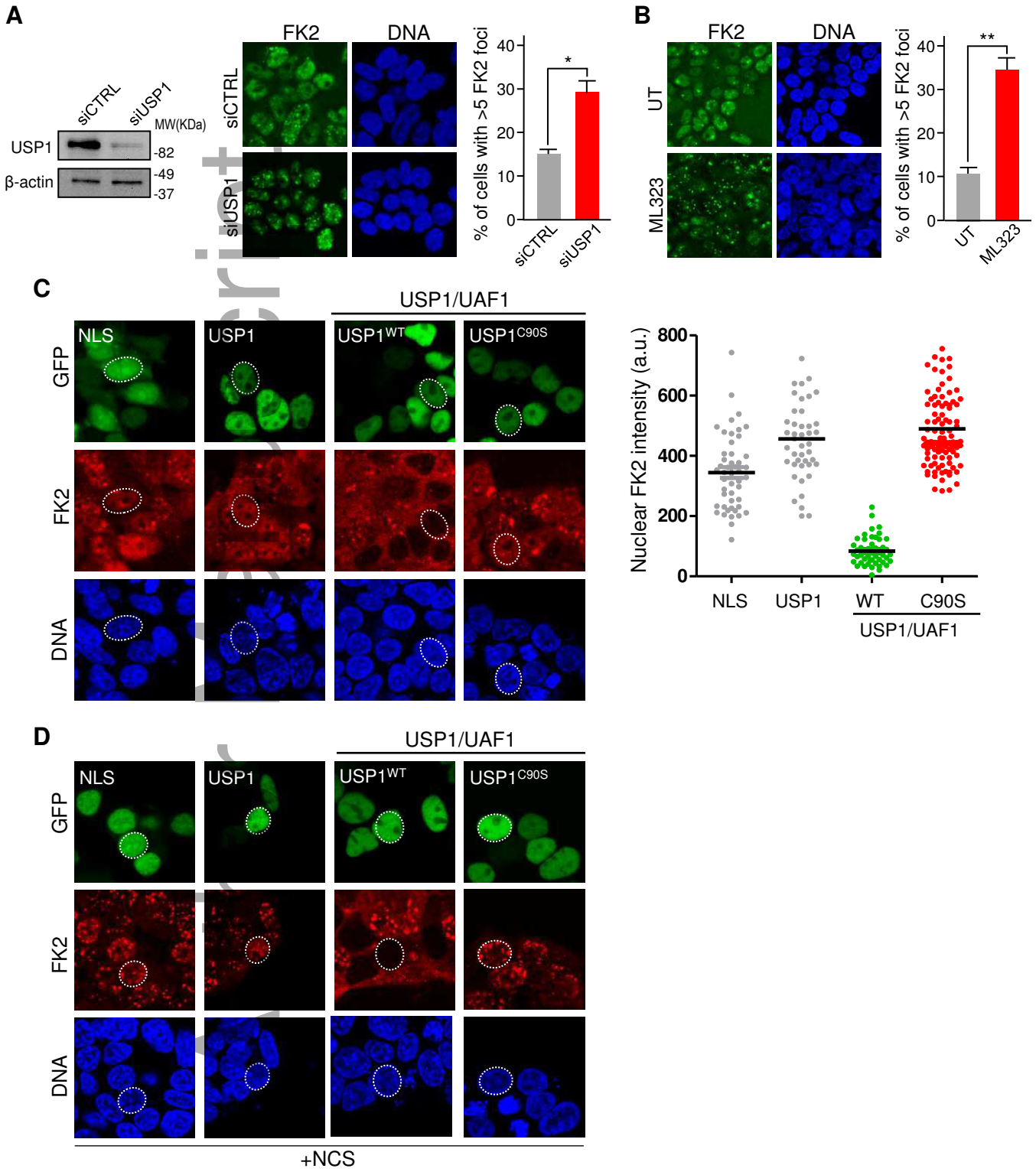

This article is protected by copyright. All rights reserved

Figure 2

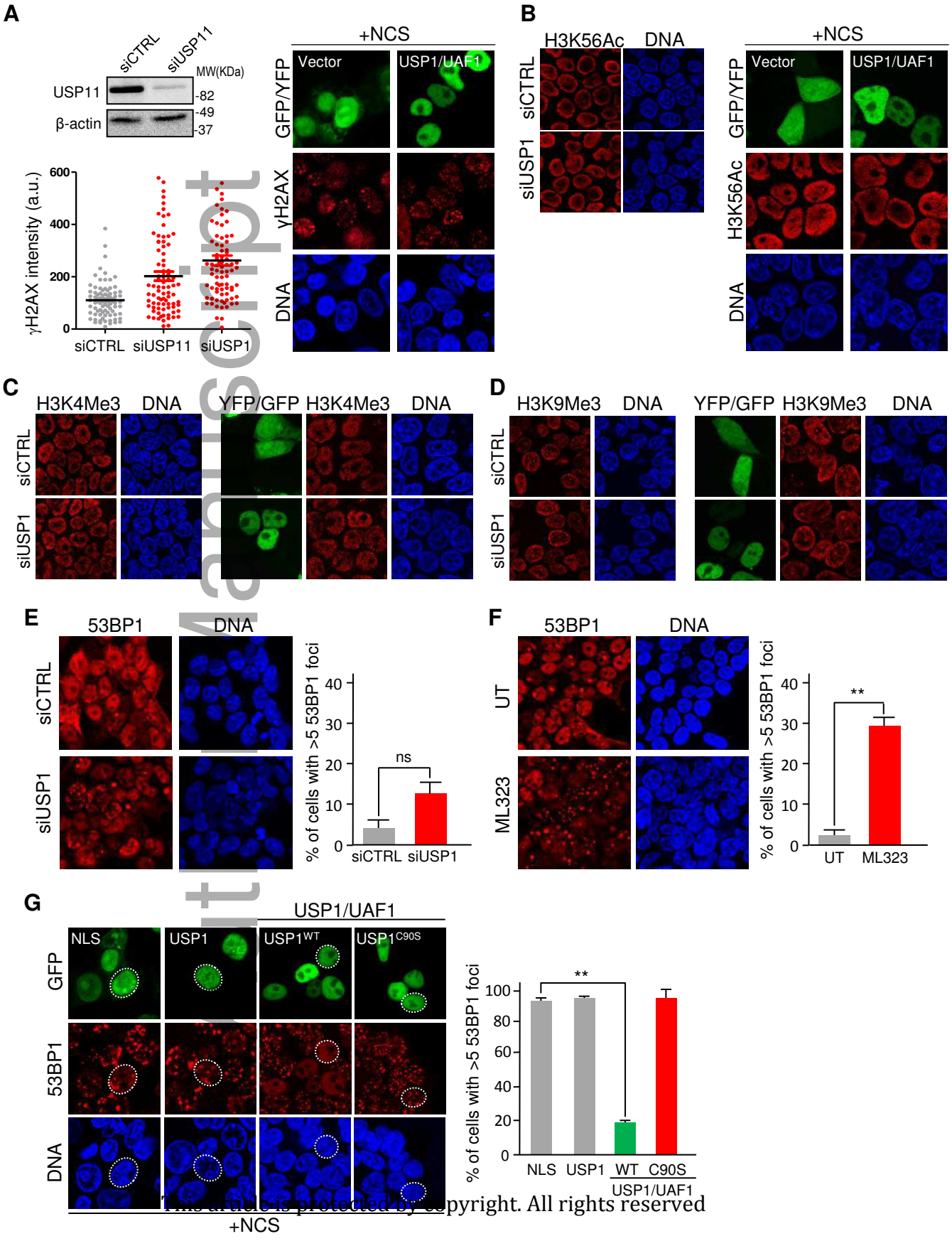

This article is protected by copyright. All rights reserved

Figure 3

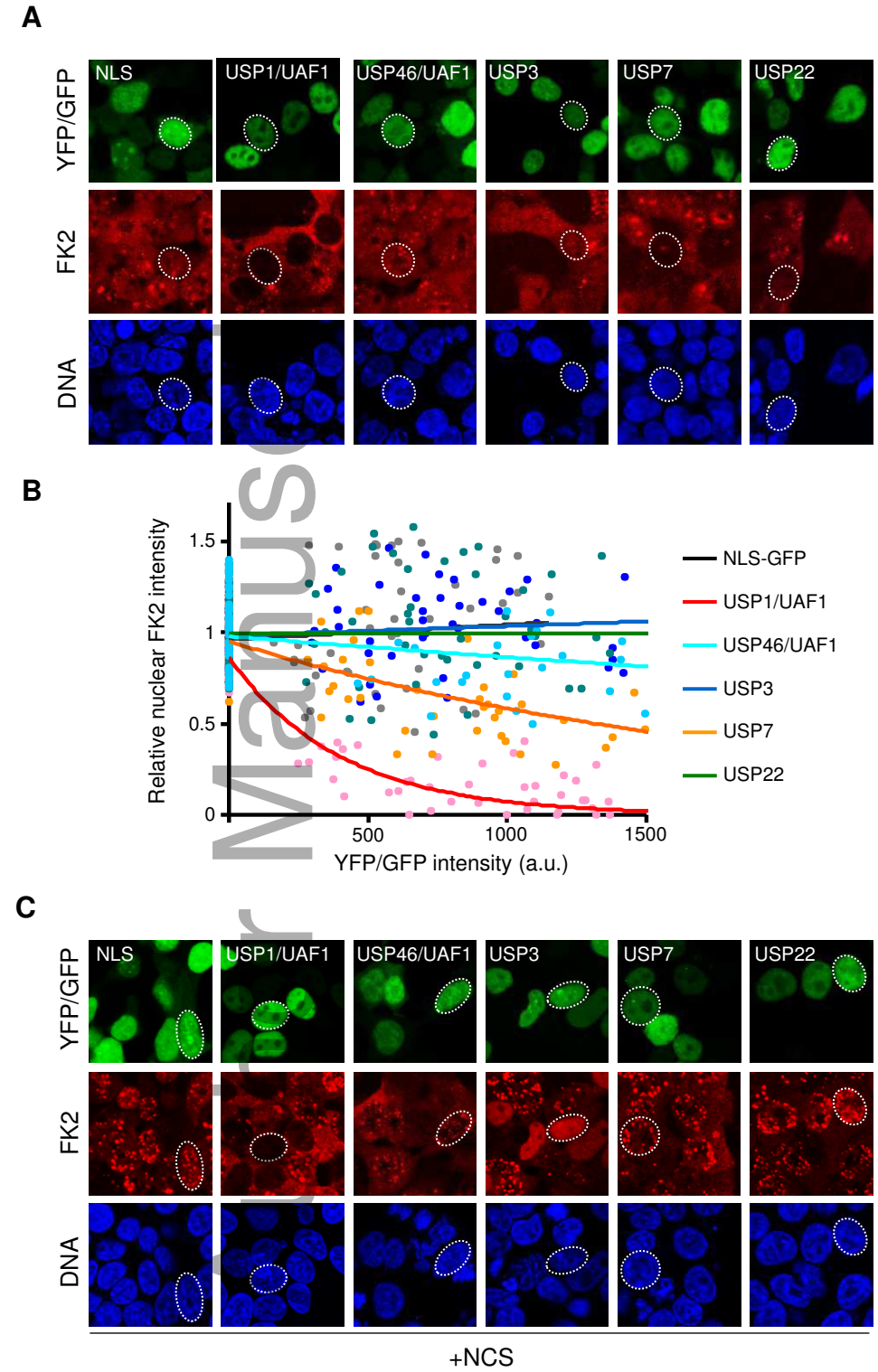

This article is protected by copyright. All rights reserved

Figure 4

febs_13648_f4.pdf

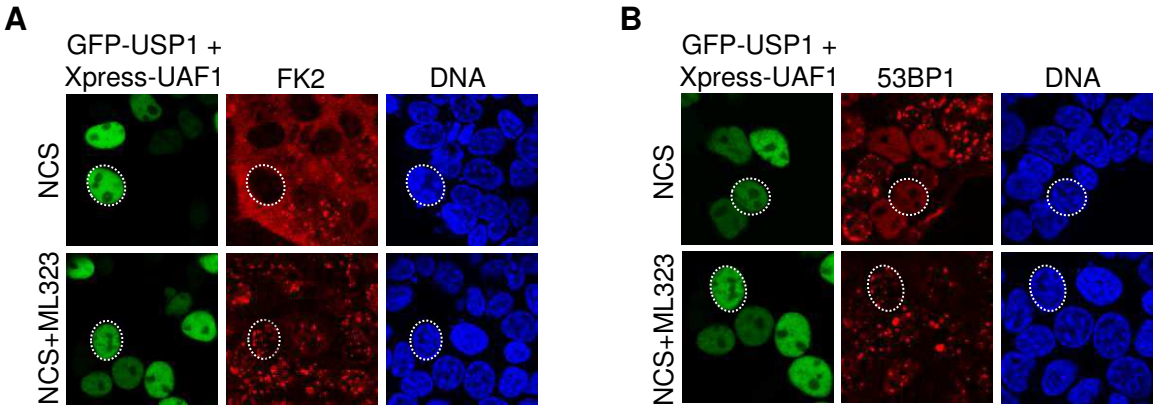

Author Manuscr

This article is protected by copyright. All rights reserved

Figure 5

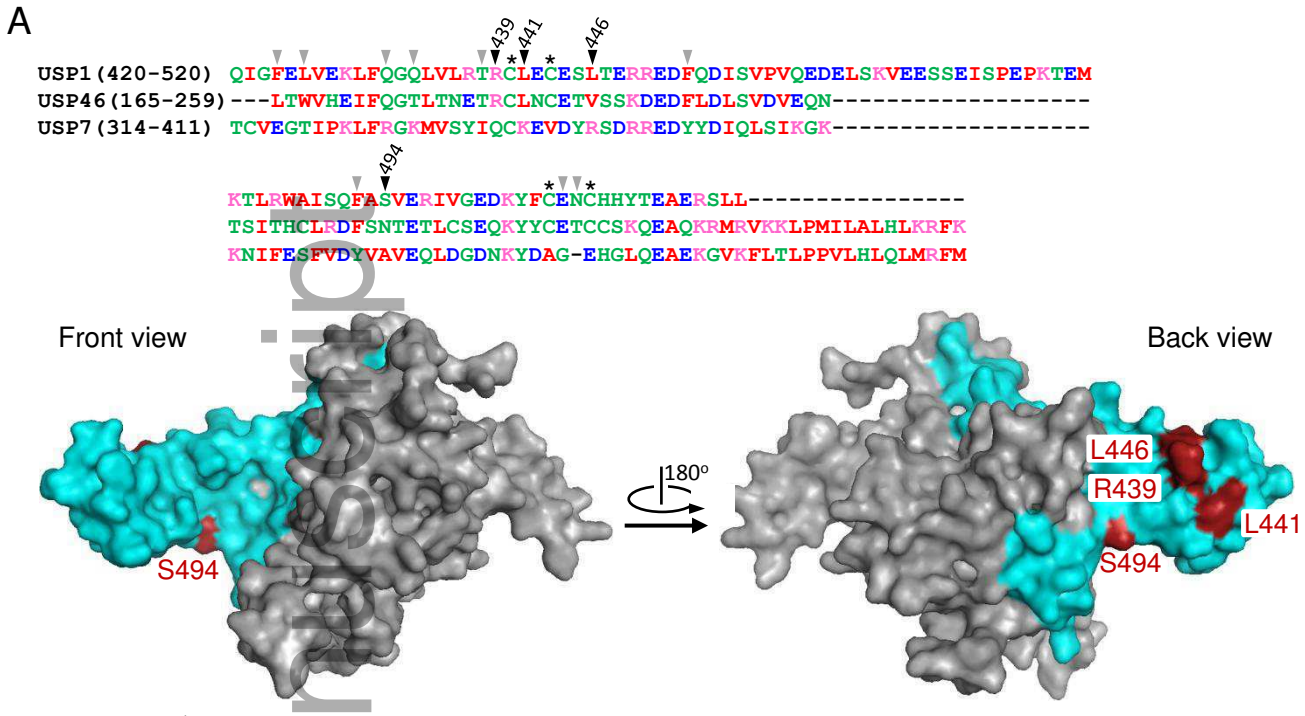

Mutant USP1^{4m}: R439Q; L441K; L446R; S494A

B

Mutant USP1^{VE}: V495A; E496A

Mutant USP1^{IV}: I498A; V499A

Mutant USP1$^{VE/IV}$: V495A; E496A; I498A; V499A

Author Manuscript

This article is protected by copyright. All rights reserved

Figure 6

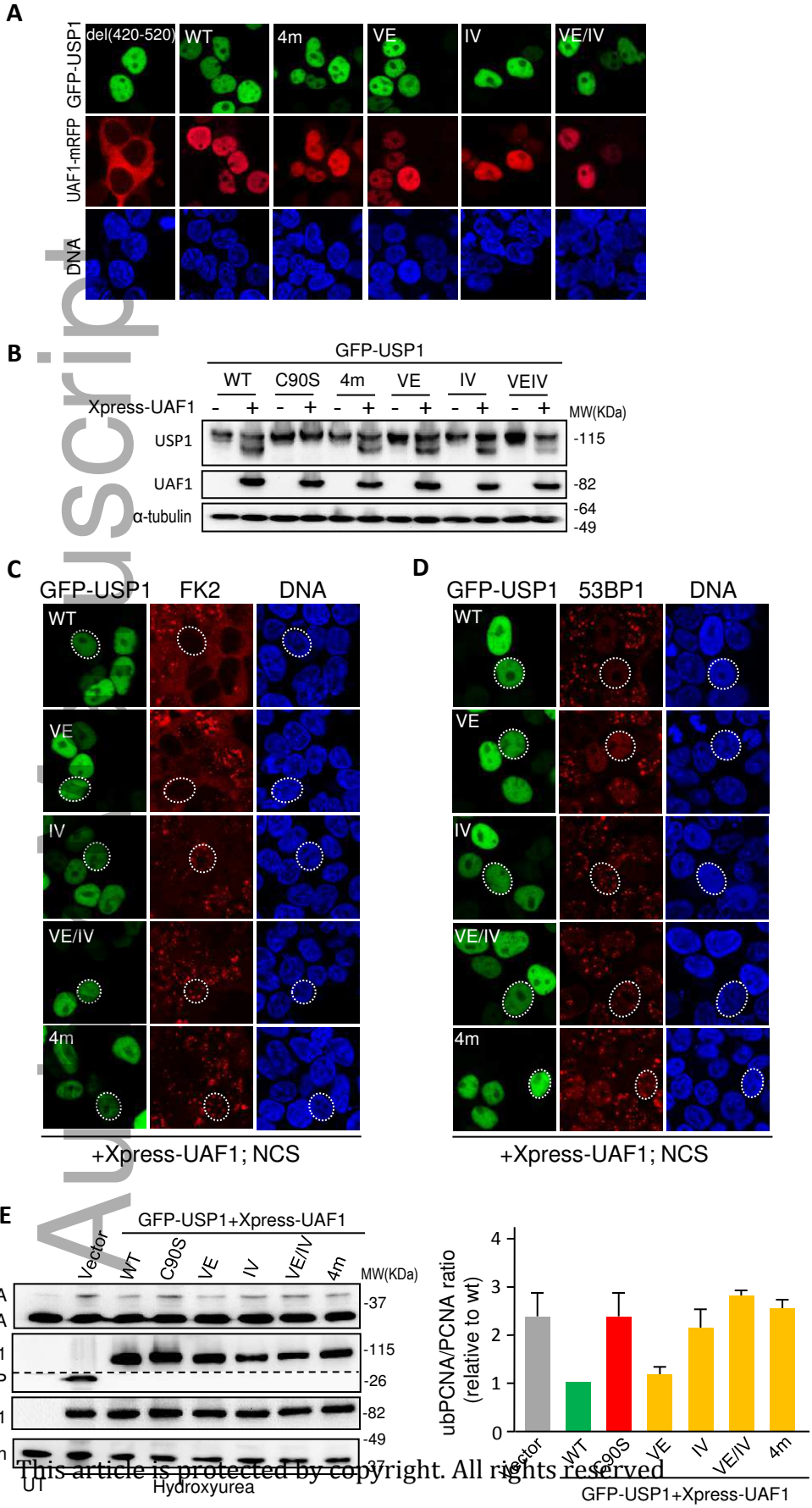

This article is protected by copyright. All rights reserved

Figure 7

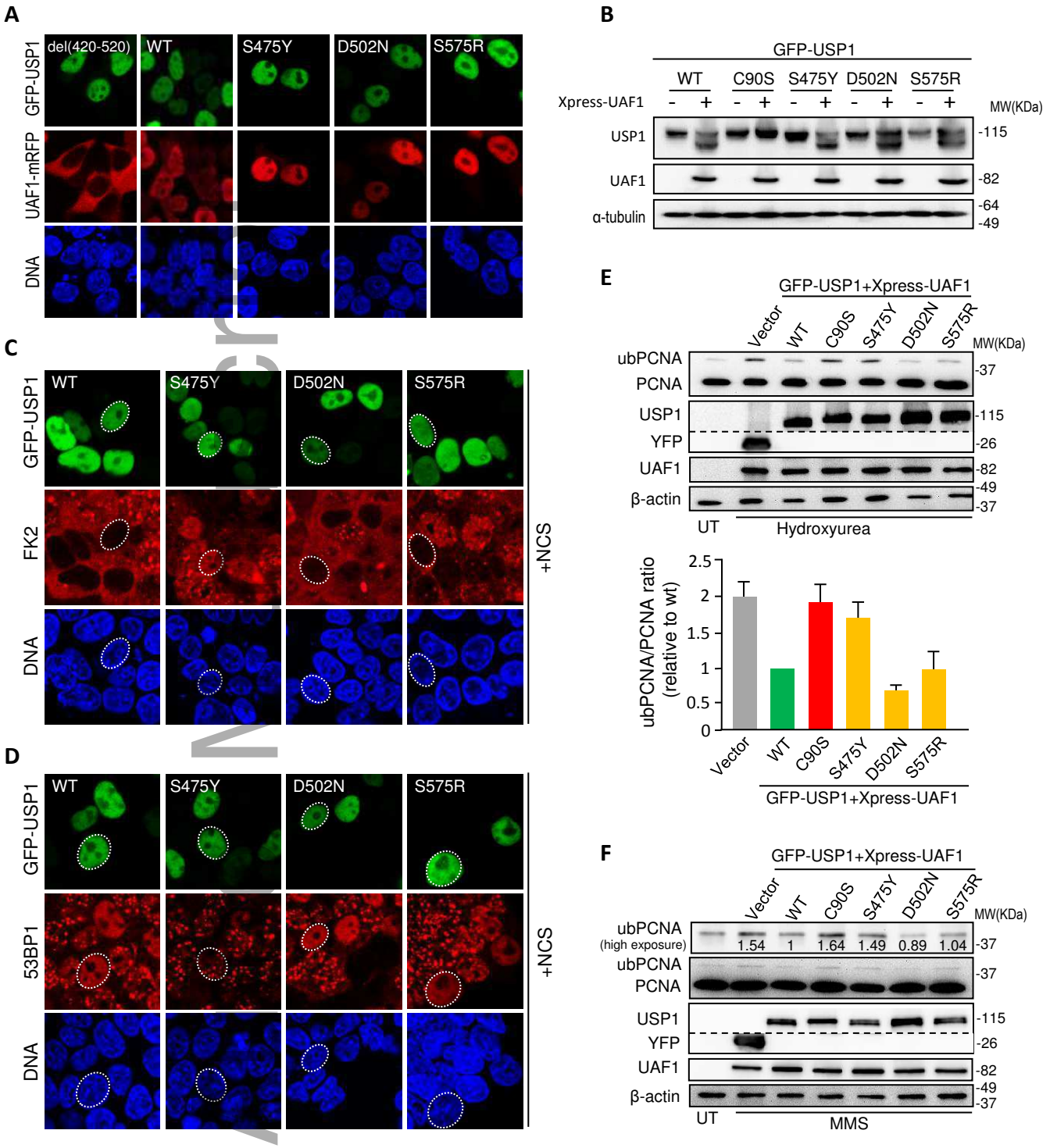

This article is protected by copyright. All rights reserved